2010

Characterization of Kaposi's Sarcoma-Associated Herpesvirus Open Reading Frames 58 and 27

Jennifer L. Quiceno
Seton Hall University

Characterization of Kaposi's sarcoma-associated herpesvirus open reading frames 58 and 27

By:
Jennifer L. Quiceno

Submitted in partial fulfillment of the requirements for the
Degree of Master of Science in Microbiology from the
Department of Biological Sciences of Seton Hall University
August, 2010

Acknowledgements

I would like to extend my thanks and gratitude to the following people:

Dr. Anne Pumfery, my mentor, for allowing me to perform research in her lab. She made it an enjoyable and wonderful learning experience. I have gained a great deal of skills from Dr. Pumfery ranging from experimental procedures to writing grants. Thank you for understanding I have a full time job and making every effort possible to accommodate me when I needed your help and guidance throughout my research. Furthermore, I would also like to thank her for her endless patience, expertise and support.

Dr. Tina Chu for her taking time out of her schedule to share in my thesis experience and for being on my defense committee.

Dr. Angela Klaus for her time and guidance in lab, as well as for sitting on my defense committee.

Erin St.Angelo, Jennifer DeCotiis, William DeCotiis, and my other fellow graduate and undergraduate lab members who have made being in the lab fun and enjoyable but also for helping to contribute to this project.

I also would like to extend my thanks to The Seton Hall Biological Sciences Department faculty. I have learned a great deal from all of you.

My family and friends, especially my husband, Stephen McGuire. His emotional support, love and encouragement helped me through my graduate career.

Table of Contents

List of Tables and Figures

Abstract

Kaposi's sarcoma-associated herpesvirus is an enveloped virus that contains glycoproteins which enable viral spread from host to host, attachment to the host cell, and host specificity. Herpesviruses are made up of different subfamilies including: alpha, beta and gamma and specific glycoproteins are conserved among the subfamilies. It has been observed that the murine gamma-herpesvirus 68 (MHV-68) contains an open reading frame (ORF) 27 which encodes a type II transmembrane glycoprotein. MHV-68 ORF27 is expressed on the outside of infected cells but is found intracellularly when expressed alone in cells. Another ORF found in MHV-68, ORF58, was discovered to be essential in the proper translocation of MHV-68 ORF27 from the cytoplasm of the cell to the surface of the infected cell. ORF58 deficient cells revealed that ORF27 was produced in typical amounts but was located to the endoplasmic reticulum. When both genes were co-expressed they formed a protein complex which reached the cell surface. There is nucleotide sequence homology between MHV-68 ORF27 and KSHV ORF27 (42% similarity), and between MHV-68 ORF58 and KSHV ORF58 (41% similarity) suggesting the proteins would have similar functions. In this study, I will attempt to investigate the localization and co-localization of KSHV ORF27 and KSHV ORF58 when expressed alone and together. KSHV ORF27 and ORF58 plasmid constructs were transfected into Vero cells and localization of ORF27 was observed within the cytoplasm of the cell using immunofluorescence. KSHV ORF58 protein was not expressed properly; therefore, localization within the cell was not observed. Further experiments must be carried out to determine what is happening to the KSHV ORF58 protein.

Introduction

Dr. Moritz Kaposi first documented purple lesions affecting elderly men, particularly of Mediterranean decent, in 1872, and since then the disease associated with these lesions, known as endothelial neoplasms, is referred to as Kaposi's sarcoma (KS) (Dourmishev *et al.*, 2003). A new human herpesvirus was discovered within the lesions of KS patients and was termed Kaposi's sarcoma-associated herpesvirus (KSHV), also known as human herpesvirus 8 (Chang*et al.*, 1994). KSHV DNA has been isolated from people suffering from KS, multicentric Castleman's disease (MCD) and primary effusion lymphoma (PEL) (Ablashi *et al.*, 2002).

KS is a vascular tumor made up of many different cell types including endothelial cells, erythrocytes, inflammatory cells and elongated endothelial cells known as "spindle" cells (Dourmishev *et al.*, 2003; Lint *et al.*, 2009). Red blood cells are often present in the lesions and are found between the spindle cells, giving the "purple" color to the lesion. As the disease progresses, the spindle cells ultimately are the major cell population at which point they begin to compress the vascular slits causing the lesions to become nodular (Ablashi *et al.*, 2002). KSHV was found 95% of the time in vascular endothelial cells and "spindle" cells of KS lesions (Ablashi *et al.*, 2002; Russo *et al.*, 1996; Wen *et al.*, 2010).

KSHV has been associated with all four forms of KS, which are classified as: classic (Mediterranean region), epidemic (AIDS-associated), endemic (African region) and iatrogenic (transplant recipients) (Ablashi *et al.*, 2002; Dourmishev *et al.*, 2003). Classic KS, described by Dr. Kaposi, usually occurs in Mediterranean/Eastern European

elderly men (Hengge *et al.*, 2002b). KS occurrence in the Mediterranean is about ten-fold higher than Europe and the United States (Dourmishev *et al.*, 2003). The lesions and nodules are normally located on the extremities of the body with little involvement of internal organs or lymph nodes (Hengge *et al.*, 2002b).

AIDS-associated KS can spread both viscerally and through the lymph system more so than any other form (Wen *et al.*, 2010). Approximately 30% of AIDS patients exhibited KS as the first symptom of AIDS (Greene *et al.*, 2007); as a result, KS was considered an AIDS defining illness (Wen *et al.*, 2010). AIDS-KS affects the skin, lymph nodes, and may also include lungs, gastrointestinal tract, liver and spleen (Ablashi *et al.*, 2002). AIDS-KS is usually found on the head and neck and develops rapidly (Dourmishev *et al.*, 2003). KS lesions can become tumors and visceral diffusions, which can lead to organ failure and finally death (Dourmishev *et al.*, 2003). KS is still the most prevalent AIDS-associated cancer in the world (Wen *et al.*, 2010).

Endemic KS is traditionally found throughout Eastern and Central Africa, and it affects younger and older people (Wen *et al.*, 2010). It is found in four distinct disease patterns: similar to classic KS; a more aggressive form invading soft tissue and bone; florid mucocutaneous and visceral disease; and fulminant lymphadenopathic disease which quickly progresses to lymph nodes and visceral organs (Hengge *et al.*, 2002b). The more aggressive form of endemic KS commonly afflicts children and has a very high mortality rate (Wen *et al.*, 2010).

The final form of KS is post-transplant/iatrogenic KS. Post-transplant KS occurs after the immune system has been suppressed for a long period of time by the therapy

used to avoid rejection of a transplanted organ (Wen *et al.*, 2010). Iatrogenic KS may become chronic or even progress quickly, but spontaneous remission will most likely occur after removal of immunosuppressive drugs (Hengge *et al.*, 2002b).

KSHV has also been strongly associated with two B cell diseases, PEL and multicentric Castleman's disease (MCD) (Lint *et al.*, 2009). KSHV viral DNA was found in lymphomas, a cancer of the lymphatic system, within the body cavities of AIDS patients and were referred to as body cavity-based lymphomas (BCBL), also known as primary effusion lymphoma (PEL) (Ablashi *et al.*, 2002; Wen *et al.*, 2010). PEL operates as a classic tumor in that every cell carries KSHV DNA (Chen *et al.*, 2007; Lint *et al.*, 2009). The lymphomas contain high copy numbers of viral DNA—anywhere from 50 to 150 KSHV episomes per infected cell (Wen *et al.*, 2010). The high copy number allows the virus to be identified easily by Southern blot analysis; this is unlike KS tissues which have few copies per cell and only PCR can be used for detection (Ablashi *et al.*, 2002). PEL is very rare and is observed in the last stages of AIDS (Lint *et al.*, 2009). It is identified by over growth of malignant B cells in the body cavity primarily in the pleura, pericardium and peritoneum (Chen *et al.*, 2007; Lint *et al.*, 2009; Wen *et al.*, 2010). PEL is aggressive and progresses rapidly leading to high mortality rates. Survival after diagnosis can typically be anywhere from two to five months (Ablashi *et al.*, 2002; Chen *et al.*, 2007; Wen *et al.*, 2010).

Castleman's disease is a rare lymphoproliferative disease typically depicted as a polyclonal, non-neoplastic disorder (Wen *et al.*, 2010). The most common form is the hyaline vascular type described as a solitary localized mass usually in a lymph node, that

can be surgically removed (Ablashi *et al.*, 2002; Lint *et al.*, 2009). The second and more aggressive form, known as the plasma cell type, is associated with widespread lymphadenopathy (Hengge *et al.*, 2002a; Wen *et al.*, 2010). MCD is most commonly seen in AIDS patients and is characterized by germinal center expansion and vascular endothelial proliferation in the lymph nodes (Wen *et al.*, 2010). KSHV is present in virtually all cases of AIDS-related MCD (Ablashi *et al.*, 2002; Lint *et al.*, 2009). It is common for MCD patients to develop KS and non-Hodgkin's lymphoma as well, but KSHV is almost always present even if KS does not develop (Ablashi *et al.*, 2002).

Many people are infected with KSHV but its seroprevalence in the population differs among the affected groups. In African countries, KSHV is observed in about 40 to 60% of the general population reaching a high prevalence rate (Lint *et al.*, 2009). The endemic areas have primary infection of KSHV occurring in childhood, and the number of infected individuals increases with age (Pelser *et al.*, 2009). Transmission of the virus in endemic regions is primarily driven within the family, from parent to child and between family members. The most likely transmission method is salivary exchange (Ablashi *et al.*, 2002; Lint *et al.*, 2009). The Mediterranean populations are found to have anywhere from 10 to 25% seroprevalence of the virus, which is why classic KS is most often diagnosed in the regions surrounding the Mediterranean (Ablashi *et al.*, 2002). The prevalence of KSHV in the rest of the world ranges from two to five percent, and is spread like a sexually transmitted disease despite the low viral load in semen of infected individuals (Ablashi *et al.*, 2002; Lint *et al.*, 2009).

Herpesviridae

The herpesvirus virion is made up of four major components: a nucleoprotein core which encapsulates a double-stranded linear DNA genome; an icosahedral capsid which surrounds the core; an unstructured dense protein layer, referred to as the tegument; and a lipid envelope containing different viral glycoproteins (Lint *et al.*, 2009; Zhu *et al.*, 2005). Production of viral DNA and assembly of the capsid occur in the nucleus of the infected cell. During herpesvirus infection, virus-specific areas are created in the nucleus, designated as replication compartments. These compartments are where viral DNA replication, late gene expression and encapsidation of progeny genomes occur. These compartments cause the formation of basophilic nuclear inclusion bodies, which is a diagnostic feature of herpesvirus infection. Production of virion particles is usually accompanied by death of the infected cell (Lint *et al.*, 2009).

The *herpesviridae* family is made up of three subfamilies designated as α, β and γ. The α-herpesviruses are grouped together based on their variable host range, short reproductive cycle, efficient destruction of infected cells, and ability to establish latent infections primarily in sensory ganglia (Knipe *et al.*, 2001). The human herpes viruses (HHV) in the alpha subfamily include: HHV1, HHV2 and HHV3 (Knipe *et al.*, 2001). The β-herpesviruses are characterized by their long reproductive cycle, slow progression of infection in culture, and possible enlargement of infected cells (Knipe *et al.*, 2001). The human herpes viruses in the beta subfamily include: HHV5, HHV6 and HHV7 (Knipe *et al.*, 2001). The γ-herpesviruses are grouped together based on their capability to replicate in epithelial cells, establish either latency or lytic infections in lymphocytes,

and cause cancer (Knipe *et al.*, 2001; Lint *et al.*, 2009). There are two genera in the γ-herpesvirus subfamily: the lymphocryptovirus genus, which includes Epstein-Barr virus (EBV), and the rhadinovirus genus, which includes: HHV4, KSHV and murine herpes virus 68 (MHV-68) (Knipe *et al.*, 2001; Lint *et al.*, 2009). The γ-herpesviruses are known to establish viral infection and evade detection by actively suppressing apoptosis and escaping immune detection (Wen *et al.*, 2010). They can alter cell cycle progression, apoptosis and immune surveillance allowing the virus to increase its odds of survival (Wen *et al.*, 2010).

KSHV Life Cycle

The KSHV genome is approximately 165 kb long, contains more than 81 open reading frames (ORF), and can encode up to 90 viral proteins (Russo *et al.*, 1996). The linear double stranded DNA viral genome has a central region with a low GC make up known as the long unique region (LUR); this region is flanked on both ends by terminal repeats (TR) which are highly GC rich (Hengge *et al.*, 2002a; Russo *et al.*, 1996; Wen *et al.*, 2010). Even though numerous ORFs of KSHV are conserved, there are KSHV specific ORFs not seen in other herpesviruses. The KSHV specific ORFs are identified as K1 to K15 (Russo *et al.*, 1996; Wen *et al.*, 2010). Attachment to a host cell is made possible by glycoproteins (gB, ORF4, gH/gL, gM/gN and gpK8.1A) binding with receptors like heparan sulfate (HS), DC-SIGN (dendritic cell-specific intercellular adhesion molecule 3 (ICAM-3)-grabbing non-integrin), integrins and other unknown ligands found on the surface of the cell (Akula *et al.*, 2001; Rappociolo *et al.*, 2006). Binding to receptors leads to the start of signaling pathways that will either cause fusion

of the virion envelope to the cell membrane or endocytosis of the virion (Chandran *et al.*, 2010; Greene *et al.*, 2009).

The pathway of entry is dependent on the cell type, for example, clathrin-mediated endocytosis has been observed in endothelial, epithelial and fibroblast cells (Akula *et al.*, 2003; Chandran *et al.*, 2010; Greene *et al.*, 2009). Attachment and entry is then followed by transportation of the endocytotic vesicle, containing the virion, to the nucleus (Raghu *et al.*, 2009). Similar to other herpesviruses, DNA replication occurs via the rolling circle mechanism in the replication compartments in the nucleus (Knipe *et al.*, 2001). Like other herpesviruses, KSHV exhibits both latent and lytic phases in infected cells (Sharma-Walia *et al.*, 2006).

After entry into the cell, polymerized microtubules deliver the viral DNA to the nucleus (Naranatt *et al.*, 2005). At this point a latent infection is established and the viral genome is replicated as an episome (Greene *et al.*, 2007; Hengge *et al.*, 2002a; Lint *et al.*, 2009). There are very few viral genes that are expressed during latency. Some of the latent viral genes include the latent nuclear antigen (LANA/ORF73), viral cyclin (v-cyclin/ORF72), viral Fas-associated death domain (FADD) interleukin-1L-converting enzyme (FLICE) inhibitory protein (v-FLIP/K13) and kaposin (K12); all are located adjacent to one another in the genome (Chandran *et al.*, 2010; Jenner *et al.*, 2002; Pyakurel *et al.*, 2007).

During latent infection the latently expressed genes prevent apoptosis of the cell, ensure the viral genome is dispersed to progeny cells, and drive the cell cycle forward (Jenner *et al.*, 2002; Lint *et al.*, 2009; Pyakurel *et al.*, 2007). For example, LANA

competes with E2F (a transcription factor) for binding of retinoblastoma protein (Rb) (Pyakurel *et al.*, 2007) which leads to further progression of the cell cycle. V-cyclin promotes progression of the cell cycle when it binds with cyclin dependent kinase 6 which, will in turn, phosphorylate Rb (Verschuren *et al.*, 2004). Phosphorylated Rb will release bound E2F (Verschuren *et al.*, 2004). Free E2F activates the transcription of S phase genes moving the cell cycle forward (Pyakurel *et al.*, 2007; Verschuren *et al.*, 2004).

In latent cells, no infectious virus particles are being produced, but when induced into reactivation, KSHV enters the lytic phase (Wen *et al.*, 2010; Zhu *et al.*, 2005). Triggering a cell to go from latency to lytic infection is mediated by the replication and transcription activator (Rta) protein, which is a viral transcriptional activator able to induce lytic gene expression alone (Chen *et al.*, 2009; Greene *et al.*, 2007; Lint *et al.*, 2009; Nakamura *et al.*, 2003). During latency Rta expression is repressed (Greene *et al.*, 2007). It has been shown that deletion of Rta inhibits both spontaneous and chemical induction of the lytic cycle (Lint *et al.*, 2009). When the cell is triggered to enter the lytic cycle, expression of the viral genes is initiated in a sequential manner beginning with the immediate early (IE), early (E) and late (L) genes (Lint *et al.*, 2009).

The IE genes regulate the subsequent transcriptional cascade; Rta, the "switch" protein, is required to initiate the lytic replication cycle (Greene *et al.*, 2007; Wen *et al.*, 2010). The first genes to be expressed after induction encode regulators of gene expression such as ORF50, K8 and ORF45 (Jenner *et al.*, 2002). The IE gene K8 appears to balance Rta's transactivation activity (Rossetto *et al.*, 2007) and ORF45 aids in the

suppression of interferon induction (Zhu *et al.*, 2002). These IE genes are followed by E genes which assist in viral DNA replication (Lu *et al.*, 2004). L genes take part in the construction and maturation of virions (Jenner *et al.*, 2002; Lu *et al.*, 2004). Glycoproteins are late genes; they are membrane proteins found on the lipid envelope of virions (Knipe *et al.*, 2001).

Glycoproteins

Glycoproteins play a major role in cell to cell interactions including attachment and entry into host cells (Knipe *et al.*, 2001). Fusion of the virion envelope with host cell membranes is primarily mediated by viral glycoproteins; viral glycoproteins can also aid in virion egression (Subramanian *et al.*, 2010). Glycoproteins are created on membrane bound ribosomes, translocated to the endoplasmic reticulum (ER) and are typically transferred to the plasma membrane via the trans-Golgi network (TGN) (Veit *et al.*, 1996). KSHV encodes many glycoproteins which are conserved in the *herpesviridae* including: gB, gH, gL, gM and gN (Chandran *et al.*, 2010; Zhu *et al.*, 2005). KSHV also encodes unique glycoproteins which include: K1, ORF4, K8.1A, K8.1B, K14 and K15 (Chandran *et al.*, 2010; Zhu *et al.*, 2005). K8.1 gene encodes two glycoproteins produced from spliced transcripts, K8.1A and K8.1B. K8.1A is the most abundant of the two (Chandran *et al.*, 2010; Chandran *et al.*, 1998; Zhu *et al.*, 2005). Birkmann *et al.* (2001) examined the binding of K8.1 to mammalian cells using soluble K8.1 protein. It was found that both K8.1 protein derivatives are capable of binding to cell surface heparin sulfate (HS) (Ablashi *et al.*, 2002; Birkmann *et al.*, 2001; Zhu *et al.*, 2005). Furthermore, soluble HS blocked infection of endothelial cells by KSHV (Birkmann *et al.*, 2001).

Viral glycoproteins are very important in the spread and attachment of the virus particle; therefore, it is imperative that we examine all known and any possible KSHV glycoproteins.

ORF27 and ORF58

There are two other possible glycoproteins or membrane associated proteins in KSHV, ORF27 and ORF58 (Chandran *et al.*, 1998; Russo *et al.*, 1996), but their functions have not yet been determined. KSHV ORF27 is homologous to EBV BDLF2 (43.3 % similarity) and MHV-68 ORF27 (42% similarity) (May *et al.*, 2005a; Russo *et al.*, 1996). BDLF2 was thought to be a virion tegument protein poorly conserved among γ-herpesviruses (Johannsen *et al.*, 2004; Tarbouriech *et al.*, 2006), but was actually found to be the eleventh glycoprotein of EBV (Gore *et al.*, 2009). BDLF2 encodes a transmembrane domain protein with N-linked glycosylation sites which classifies BDLF2 as a type II envelope glycoprotein (Gore *et al.*, 2009). MHV-68 ORF27 was also found to be a glycoprotein, analogous to BDLF2, that plays a role in cell to cell viral spread, but also restricts host antibody access to the sensitive extracellular loop of the MHV-68 ORF58 glycoprotein (May *et al.*, 2005a). Zhu *et al.* (2005) purified KSHV virions and determined all proteins present within the virion. The KSHV ORF27 protein was found in the purified virions but localization within the virion was not determined (Zhu *et al.*, 2005). Rozen *et al.* (2008) observed virion protein interactions and found KSHV ORF27 interacted with two envelope glycoproteins (ORF47 and ORF53) and ORF45, a tegument protein. After examination of KSHV ORF27 homologues and its association with purified virions, I hypothesize that KSHV ORF27 is a possible glycoprotein.

KSHV ORF58 is homologous to EBV BMRF2 (50.6 % similarity) (Russo *et al.*, 1996) and MHV-68 ORF58 (41 % similarity) (May *et al.*, 2005a). BMRF2, a highly hydrophobic multi-spanning transmembrane protein, has been observed to be crucial to EBV infection of epithelial cells (Tarbouriech *et al.*, 2006; Xiao *et al.*, 2007). An arginine–glycine–aspartic acid (RGD) motif was discovered in the main extracellular loop of BMRF2 (Xiao *et al.*, 2009). RGD motifs interact with many extracellular matrix proteins that interact with host cell surface integrins (Akula *et al.*, 2002). The interactions with integrins can activate many integrin associated pathways which could lead to virion attachment and entry or cell to cell spread (Xiao *et al.*, 2007). BMRF2 was not crucial to the egress of infectious EBV particles, supporting the idea that the protein may actually help in cell to cell spread (Loesing *et al.*, 2009; Xiao *et al.*, 2008). EBV BMRF2 protein has been observed in mature virions (Xiao *et al.*, 2007). MHV-68 ORF58 also encodes a type II multi-membrane spanning protein which can bind to cells via an extracellular loop (EC4), similar to the RGD containing loop found in BMRF2 (May *et al.*, 2005a; Xiao *et al.*, 2009). KSHV ORF58 encodes a highly hydrophobic protein which has many potential transmembrane regions (Chan *et al.*, 1998). KSHV ORF58 was predicted to be a type IIIa or IIIb plasma membrane associated protein (Chan *et al.*, 1998). The similarities between the ORF58 homologues lead us to speculate that KSHV ORF58 protein may also be a glycoprotein.

Identifying the expression patterns of ORF27 and 58 may help in understanding their role in the virus life cycle. Gene expression patterns can be determined using many different techniques. The various methods will help to determine the true expression

pattern of a gene. Nakamura *et al.* (2003) developed a multiprobe RNase protection assay to examine all KSHV genes expression patterns after induction. Yoo *et al.* (2005) established an infection in endothelial cells using a recombinant KSHV expression vector; and whole genome RT-qPCR was then used to evaluate expression patterns of KSHV transcripts after infection. Anti-viral drugs can also be used to study expression patterns. Lu *et al.* (2004) used cidofovir (CDV), an inhibitor of viral DNA replication, to examine KSHV gene expression. CDV will cause inhibition of viral DNA synthesis and replication by being incorporated into the replicating DNA which terminates the strand (De Clercq *et al.*, 2003). CDV allows for the detection of late viral transcripts, which would rely on viral DNA replication, from other transcripts (De Clercq *et al.*, 2003).

Nakamura *et al.* (2003) found KSHV ORF27 to be late, meaning expression rate surpassed two-fold amplification after 16 hours and continued to increase. ORF27 would be expected to be expressed late in the replication cycle if it were a glycoprotein. Yoo *et al.* (2005) also observed a late expression pattern for KSHV ORF27. Lu *et al.* (2004) found ORF27 was sensitive to CDV. Many of the genes sensitive to CDV were virion structural proteins (Lu *et al.*, 2004). Ebrahimi *et al.* (2003) identified late transcripts with phosphonoacetic acid treatment (another viral DNA polymerase inhibitor) prior to infection with MHV-68. Total RNA was isolated and analyzed by DNA microarrays. MHV-68 ORF27 was identified as a late expressing transcript (Ebrahimi *et al.*, 2003). Similar to its homologues, EBV BDLF2 was also observed having a late expression pattern (Tarbouriech *et al.*, 2006).

Nakamura *et al.* (2003) found KSHV ORF58 had an immediate-early expression pattern, corresponding to a greater than or equal to two-fold increase prior to 12 hours with expression reaching its apex at 24 hours. Interestingly, ORF58 mRNA expression was not observed late in the cycle as would have been expected. Contrary to Nakamura *et al.* (2003) findings for KSHV ORF58, Yoo *et al.* (2005) determined, with the use of the KSHV recombinant expression vector, KSHV ORF58 had a late expression pattern. Lu *et al.* (2004) found KSHV ORF58 was insensitive to CDV which would mean ORF58 was not a late expressing transcript. On the other hand, Lu *et al.* (2004) observed only ~25% of genes with glycoprotein homology were CDV sensitive. The remaining glycoproteins were CDV insensitive with expression occurring early in the lytic cycle (Lu *et al.*, 2004). This early expression may allow time for post-translational modification or targeting of the protein to other locations within the cell (Lu *et al.*, 2004). EBV BMRF2 mRNA expression occurred during the lytic cycle (Loesing *et al.*, 2009; Xiao *et al.*, 2007). Ebrahimi *et al.* (2003) identified MHV-68 ORF58 as a late expressing transcript.

Sander *et al.* (2007) identified the localization patterns of KSHV ORF27 and ORF58 using expression plasmids. KSHV ORF58 was subcellularly localized in the TGN (Sander *et al.*, 2007). KSHV ORF27 was observed to throughout the cytoplasm heterogeneously (Sander *et al.*, 2007). Localization of the EBV homologues depended on the presence of other proteins (Gore *et al.*, 2009). When expressed alone BDLF2 did not travel from the ER to the TGN (Gore *et al.*, 2009; Loesing *et al.*, 2009). Yet, when it was co-expressed with BMRF2, BDLF2 co-localized and translocated to the cell membrane (Gore *et al.*, 2009). Therefore, BDLF2 translocation and correct processing is

dependent on BMRF2 (Gore *et al.*, 2009; Loesing *et al.*, 2009). Studies show that BDLF2 and BMRF2 form a stable complex (Gore *et al.*, 2009; Xiao *et al.*, 2009). Correct processing of MHV-68 ORF27 and its transportation from the ER to the cell plasma membrane also only occured when co-expressed with MHV-68 ORF58 (May *et al.*, 2005a), similar to the EBV BDLF2 protein. In cells expressing only MHV-68 ORF27, the protein was localized strictly within the cell at the ER (May *et al.*, 2005a). MHV-68 ORF27 and ORF58 also form a protein complex that aids in cell to cell spread of the virus (May *et al.*, 2005a).

KSHV ORF27 and ORF58 sequence homology to EBV and MHV-68 suggests their functions may also be similar. In order to investigate this hypothesis, KSHV ORF27 and ORF58 were cloned. ORF27 fusion protein was expressed in mammalian cells. After expression was verified via western blot analysis, ORF27 fusion protein was visualized using confocal microscopy to illustrate localization of ORF27 in the cytoplasm of the cell.

Materials and Methods

Sequence Alignment

KSHV ORF27, EBV BDLF2 and MHV68 ORF27 were aligned using ClustalW2, (http://www.ebi.ac.uk/clustalw2/), using the following accession numbers: KSHV ORF27 - AAC57108.1, EBV BDLF2 - CAD53445.1, MHV68 ORF27 - AAB66398.1. KSHV ORF58, EBV-BMRF2 and MHV68 ORF58 were also aligned using the ClustalW2 program. The following accession numbers were used in the ORF58 alignment: KSHV ORF58 - AAC57143.1, EBV-BMRF2 - CAD53408.1, MHV68 ORF58 - AAB66448.1. The protein sequences of the ORF27 homologues were also analyzed for possible N-linked glycosylation sites using NetNGlyc 1.0 Server, a prediction program (Blom *et al.*, 2004). http://www.cbs.dtu.dk/services/NetNGlyc/

Cloning of ORF 58 and 27

KSHV ORF58 was cloned into p3XFLAG-CMV-14 (Sigma-Aldrich) and p3XFLAG-CMV-26 (Sigma-Aldrich). KSHV ORF27 was cloned into phCMV2 (Genlantis). Gene inserts were amplified using PCR. Body-cavity-based lymphoma cell line (BCBL-1) genomic DNA was used as the template. The thermocycler conditions for denaturation, annealing and extension are listed on Table 1, 30 cycles were used to amplify the genes. The polymerase chain reaction (PCR) consisted of the following: 50 ng/ µl BCBL-1 template DNA, 50 pmol of primer mix, 10 mM dNTP mix, 1X PCR Buffer (USB) and 1 µl FideliTaq DNA Polymerase (USB) in a 50 µl reaction with RNase free water, some reactions had an additional 1 mM $MgCl_2$. PCR products were then

electrophoresed on a 1.0% (w/v) agarose gel in 1X Tris-acetate-EDTA buffer (TAE; 400 mM Tris-acetate, 10 mM EDTA) containing 0.5 μg/ ml ethidium bromide. The PCR products were then gel purified using the QIAquick Gel Extraction Kit (Qiagen) according to manufacturer's instructions.

All purified PCR products and vector plasmids were digested with *Bgl* II (Promega) and *Eco* RI (Promega) restriction enzymes. After digestion, PCR products and vectors were purified using the Charge Switch Kit (Invitrogen) before ligation. The ligation reaction consisted of T4 DNA ligase (Promega), 1X ligase buffer (Promega), purified PCR and plasmid products (double digested) in a total volume of 20 μl. Control ligations, which did not include the gene of interest, were also prepared. The ligation reactions were then incubated overnight at 16°C. The ORF58/27 constructs were then transformed into *Escherichia coli* (*E. coli*) DH5α cells (described in detail below). Colonies from the transformation were grown in Luria broth (LB) with ampicillin or kanamycin (100 μg/ μl), depending on the plasmid used, overnight at 37°C. The plasmid-insert construct DNA was then isolated from the overnight cell culture using Quantum Prep Plasmid mini-prep kit (Bio Rad). The isolated DNA was double digested with the appropriate restriction enzymes and the reaction was electrophoresed in a 1% agarose gel to check for the presence of the KSHV gene inserts. To verify the inserts were correctly cloned the presumptive positive clones were sent to Genewiz (http://www.genewiz.com/) for sequencing.

Insert	3′ primer	5′ primer	PCR Conditions
ORF58 (C and N terminally tagged)	aaagatctggccaacaactttatttattaccg	aagaattcttgccgcctggacagtgag	94°C - 2min; 94°C - 30sec; 55°C - 30sec; 72°C - 1min
ORF58 (N terminally tagged)	aaagatctttagccaacaactttattta	aagaattcttgccgcctggacagtgag	94°C - 2min; 94°C - 30sec; 53°C - 45sec; 68°C - 1min
ORF58 (C terminally tagged)	aaagatctggccaacaactttatttattaccg	aagaattcaccatgtgccgcctggacagtgag	94°C - 2min; 94°C - 30sec; 61°C - 45sec; 68°C - 1min
ORF27	atgaattcaccagtgacacaccttta	aaagatcttgcgtcatctgatattctg	94°C - 2min; 94°C - 30sec; 47°C - 30sec; 72°C - 1min

Table 1: List of ORF58 and ORF27 primers and their respective PCR conditions. Virus specific sequence is underlined and the sequence of the restriction enzyme sequence is in red.

Transformation

Frozen *E. coli* DH5α competent cells were thawed on ice, gently mixed and 50 µl aliquots were transferred into labeled tubes. The ligation reactions, five µl each, were then added to the dispensed cells and gently mixed. The ligation/cell mixture was incubated on ice for 30 minutes. The cells were then heat shocked at 42°C for 60 seconds and then placed on ice for two minutes. After resting on ice, 450 µl of LB was added to the transfected cells. The cells were then transferred to a 37°C water bath for one hour. The appropriate volume (100-200 µl) of transformed cells were spread on LB agar plates containing either ampicillin or kanamycin (100 µg/ µl) and incubated at 37°C overnight.

Transfection

Vero, African green monkey kidney, cells were plated at a concentration of $2.0x10^5$ cells/well and incubated for 24 hours at 37°C/5% CO_2 in two ml of Dulbecco's

Modified Eagle Medium (DMEM) (Mediatech Inc) supplemented with 1% penicillin-streptomycin (Mediatech Inc) and 10% fetal bovine serum (PAA laboratories). Transient transfection was carried out using GeneJuice (Novagen) according to manufacturer's instructions. A mixture of Genejuice (three µl) and serum free DMEM (100 µl) was created for each variable. The tubes were then incubated at room temperature for five minutes. Afterwards, one µg of extracted clone DNA was added to the appropriately labeled DMEM/Genejuice mixture and incubated 15-20 minutes at room temperature. After incubation, DMEM/Genejuice/clone DNA mixtures were added to Vero cells and cells were grown for 48 hours at 37°C/5% CO_2.

Protein Extraction

Forty eight hours post-transfection, cells were rinsed with phosphate buffer saline (PBS). Lysis buffer [50 mM Tris-HCl (pH 7.5), 120 mM NaCl, 5 mM EDTA, 0.5% NP-40, 50 mM NaF, 0.2 mM Na3VO4, 1 mM DTT, 1 mM PMSF or 1 Complete protease cocktail tablet (Roche) with 1 mM DTT] was then added to the adherent cells in the well. After addition of the lysis buffer, cells were scraped with a plastic scraper and placed into a microcentrifuge tube on ice. The scraped cells were then incubated on ice for ten minutes with periodic vortexing. Cells were then centrifuged (12,000 rpm) at 4°C for ten minutes. The supernatant was transferred to a new tube and the pellet was discarded. The extracted protein samples were stored at -80°C.

Extracted protein concentrations were calculated using a spectrophotometer. A standard curve was created using bovine gamma globulin (Bio-Rad) at increasing amounts (one, three, five, and ten micrograms) in one ml of protein determination reagent

Bradford dye (USB). The optical density for protein samples were analyzed at 595 nm. An aliquot of the extracted protein samples were added to one ml of Bradford dye and optical density was recorded at 595 nm. The gamma globulin standard curve was then used to calculate the protein concentrations of the extracted protein samples.

SDS PAGE and Western Blot

A 10% SDS PAGE gel was used to separate the protein extracts. The SDS PAGE resolving gel consisted of the following: 375 mM Tris (pH 8.8), 10% acrylamide, 0.1% SDS, 0.1% ammonium persulfate, 0.04% TEMED. The stacking gel was made up of: 5% acrylamide, 125 mM Tris (pH 6.8), 0.1% SDS, 0.1% ammonium persulfate, 0.1% TEMED. Extracted proteins were prepared with SDS loading buffer (125 mM Tris pH 6.8, 4% SDS, 20% Glycerol, 10% β-Mercaptoethanol, 200 mM DTT and 0.002% bromophenol blue) and boiled at 100°C for five minutes. Samples then were loaded and run on SDS PAGE gel at 100–150 volts. The separated proteins were then transferred onto a nylon Immobilon P membrane (Millipore) using a cathode core filled with transfer buffer (20% methanol, 0.1% SDS, 1X transfer buffer [100 mM Glycine, 12.5 mM Tris-HCl pH 8.3] and deionized water) overnight at 0.08 amps.

After the overnight transfer, the membrane was blocked with non-animal protein-blocker (NAP) (GBiosciences) diluted 1:2 in TBST (25 mM Tris-HCl (pH 8.0), 125 mM NaCl, 0.1% Tween-20). The membrane was blocked, one to four hours, at room temperature with rocking. Primary antibodies were diluted 1:1000 in 1:4 NAP/TBST (10 ml total volume) and incubated, one to four hours, at room temperature with rocking. The primary antibody used for phCMV2-ORF27 was HA.11 monoclonal antibody raised in

mouse (Covance) and the primary antibody for p3XFLAG-ORF58 was ANTI-FLAG M2 monoclonal antibody (Sigma-Aldrich) developed in either mouse or rabbit. Afterwards, the membrane was then washed four times with TBST, ten minutes each wash.

After the TBST washes the secondary antibody, anti-mouse or anti-rabbit IgG horseradish peroxidase (HRP)-linked antibody (Cell-Signaling), was diluted 1:1000 in TBST (ten ml total volume) and added to the membrane. The membrane was incubated with the secondary antibody for one to four hours at room temperature with rocking. The membrane was then washed with TBST as described previously. The ECL Plus Western Blotting Detection Reagent (GE Healthcare) was used, according to manufacturer's instructions, to detect any immobilized HRP-linked antibodies on the membrane. Finally, the membrane was scanned on the STORM Scanner 860 (Molecular Dynamics) phosphoimager to visualize the protein bands. The background and contrast levels of the scanned images were adjusted with ImageQuant 5.2.

Reverse Transcription-Polymerase Chain Reaction (RT-PCR)

Reverse transcription PCR was used to observe if ORF58 DNA was being transcribed into RNA in cells after transfection. Vero cells were transfected with ORF58 constructs as detailed above. Forty eight hours post-transfection, total RNA was extracted using RNA spin mini RNA isolation kit (GE Healthcare), according to manufacturer's instructions. RNA concentrations were quantified using a spectrophometer at 260 nm. The extracted RNA samples were diluted 1:100 in sterile water and then transferred to quartz cuvettes. The reading observed at 260 nm multiplied

by the dilution factor and 40 μg/ ml (equivalent to one A260 unit) will give the approximate concentration of RNA.

RNA samples, two μg total, were then treated with RQ1 RNase-Free DNase (Promega) for 30 minutes at 37°C. A one μl aliquot of DNase stop solution (Promega) was added to the RNA samples to terminate the DNase reaction; which was followed by 65°C incubation for ten minutes. The RNA samples (1 μg, 9.1 μl each) were incubated for ten minutes at 70°C, followed by ten minutes at 4°C. RT master mix was prepared with the RT-PCR kit (Promega) as follows (20 μl total volume): 5 mM $MgCl_2$, 1X RT buffer, 1 mM dNTP mix, 0.5 μl recombinant RNasin ribonuclease inhibitor, 0.6 μl AMV reverse transcriptase and 0.025 μg/ μl $Oligo(dT)_{15}$ primer. A "no RT" master mix was prepared without RT, RNasin and $Oligo(dT)_{15}$ primer. Samples prepared without RT, RNAsin, and $Oligo(dT)_{15}$ would identify any possible DNA contamination in the RNA samples. The RT and "no RT" master mixes were then added to the RNA samples. The reaction was then carried out at 42°C - 30 minutes, 95°C – five minutes, and 10°C over night.

PCR was then carried out with new ORF58 primers that were used to amplify a small portion of the sequence. The primers created were: 3'cagcatgctcacgaggaata, 5' tcctgattggcctggataag. GAPDH primers were used as a positive control for RT-PCR. The PCR consisted of the following: 10 μl RT reaction, 50 pmol primer mix, 25 μl Master mix (Promega) and nuclease-free water. The PCR conditions were as follows: 94°C-30 seconds, 55°C-30 seconds, 72°C-30 seconds for 30 cycles. RT-PCR reactions were then run and visualized on a 1% agarose gel.

Immunofluorescence

Coverslips and slides were acid washed in 1 M HCl solution heated at 50°-60°C for four hours, cooled to room temperature and then rinsed in 100% ethanol. Treated coverslips were placed on the bottom of wells prior to adding Vero cells. To each well, $2.0x10^5$ cells were then added and cells were grown for 24 hours at 37°C/5% CO_2. The transfections were performed as outlined above. Cells were rinsed in PBS, 48 hours post transfection, and fixed to the coverslips with 3.7% paraformaldehyde solution at 37°C/5% CO_2 for 30 minutes.

Fixed cells were then covered with blocking buffer (1% bovine serum albumin in PBS) for 30 minutes at 37°C/5% CO_2. Blocking buffer was then removed and the primary HA-Tag rabbit monoclonal antibody (Cell Signaling) was added to the coverslips. Coverslips were incubated one hour at room temperature and subsequently washed three times in PBS. Transfected cells were then incubated with secondary antibody conjugated to a fluorochrome Alexa floura 488 rabbit IgG (Invitrogen) for ORF27. Cells were incubated one hour at room temperature then washed three times with PBS. DAPI stain solution was then added to cells for five minutes at room temperature. Each coverslip was then inverted onto a slide containing ten µl of Cytoseal mounting media (Richard-Allan Scientific). Any excess media was removed and the edges of each coverslip were sealed with transparent nail polish. Proteins of interest were visualized using the Olympus Fluoview FV1000 confocal microscope. The argon laser was used to excite Alexa 488 fluorophore and the diode blue 405 was used to excite the DAPI stain.

Results

ORF27 and ORF58 sequence comparisons

In order to determine ORF27 and ORF58 sequence similarities to EBV and MHV-68, all sequences were aligned using ClustalW2, a sequence alignment program for DNA or proteins (Chenna *et al.*, 2003). EBV BDLF2 and MHV-68 ORF27 were predicted to encode type II transmembrane glycoproteins with N-linked glycosylation sites (Gore *et al.*, 2009; May *et al.*, 2005b). Figure 1A illustrates the sequence alignment between KSHV ORF27 and its homologues. Identification of the N-linked glycosylation sites were accomplished using NetNGlyc 1.0 Server, a prediction program (Blom *et al.*, 2004). The glycosylation program showed multiple N-linked glycosylation sites in the extracellular regions of all ORF27 homologues. There was also a marked difference observed in the lengths of ORF27 homologues cytoplasmic tails. The KSHV ORF27 cytoplasmic tail was 82 amino acids shorter than EBV BDLF2 and 32 amino acids longer than MHV-68 ORF27.

The ORF58 alignment was enhanced using information provided by May *et al.* (2005). EBV BMRF2, MHV-68 ORF58 and KSHV ORF58 are predicted to contain 11 transmembrane (TM) regions (May *et al.*, 2005a). We see in Figure 1B, the TM regions had high numbers of identical, conserved and semi-conserved amino acids. As per May *et al.* (2005), KSHV ORF58 protein had 11 TM domains, equivalent to both MHV-68 ORF58 and BMRF2. May *et al.* (2005) used EC4 in EBV BMRF2, the largest hydrophilic loop, as a point of reference to determine the other hydrophilic domains. The

RGD motif, within the EC4 region, is important in virion attachment and cell to cell viral spread (Xiao *et al.*, 2007). The RGD motif was not observed in either MVH-68 (ORF58) or KSHV (ORF58) (Figure 1B).

Cloning of ORF27 and ORF58

To study ORF27 and ORF58, the genes were cloned into mammalian expression plasmids. The genes were amplified using PCR and cloned into phCMV-2 and p3XFLAG-14, respectively. PCR was carried out using gene specific primers and BCBL-1 genomic DNA. Figures 2A and 2B confirm the specificity of the primers to amplify the genes of interest at the expected sizes of 874 bp for ORF27 and 1094 bp for ORF58. The bands observed were consistent with the nucleotide sequence lengths of ORF27 and ORF58 as described by Russo *et al.* (1996). After PCR and gel purification, ORF27, ORF58, and the plasmids were digested sequentially with *EcoR* I and *Bgl* II. Following double digestion, the genes and plasmids were purified and ligation was carried out. The ligated ORF27 and ORF58 plasmids were then transformed into *E. coli* strain DH5α. DNA was isolated from colonies that were picked and grown overnight. The isolated DNA was double digested with *EcoR* I and *Bgl* II. In Figures 2C and 2D we observed positive clones for both phCMV-2-ORF27 (five total) and p3XFLAG-14-ORF58 (ten total).

Selected clones were sent to Genewiz for sequencing. ORF27-C1 and C10 sequences were compared to the KSHV nucleotide sequence. KSHV ORF27-C1 had 98% identity to the published KSHV ORF27 sequence (accession number AAC57108.1) and KSHV ORF27-C10 had 96% identity (data not shown). Due to the higher percent

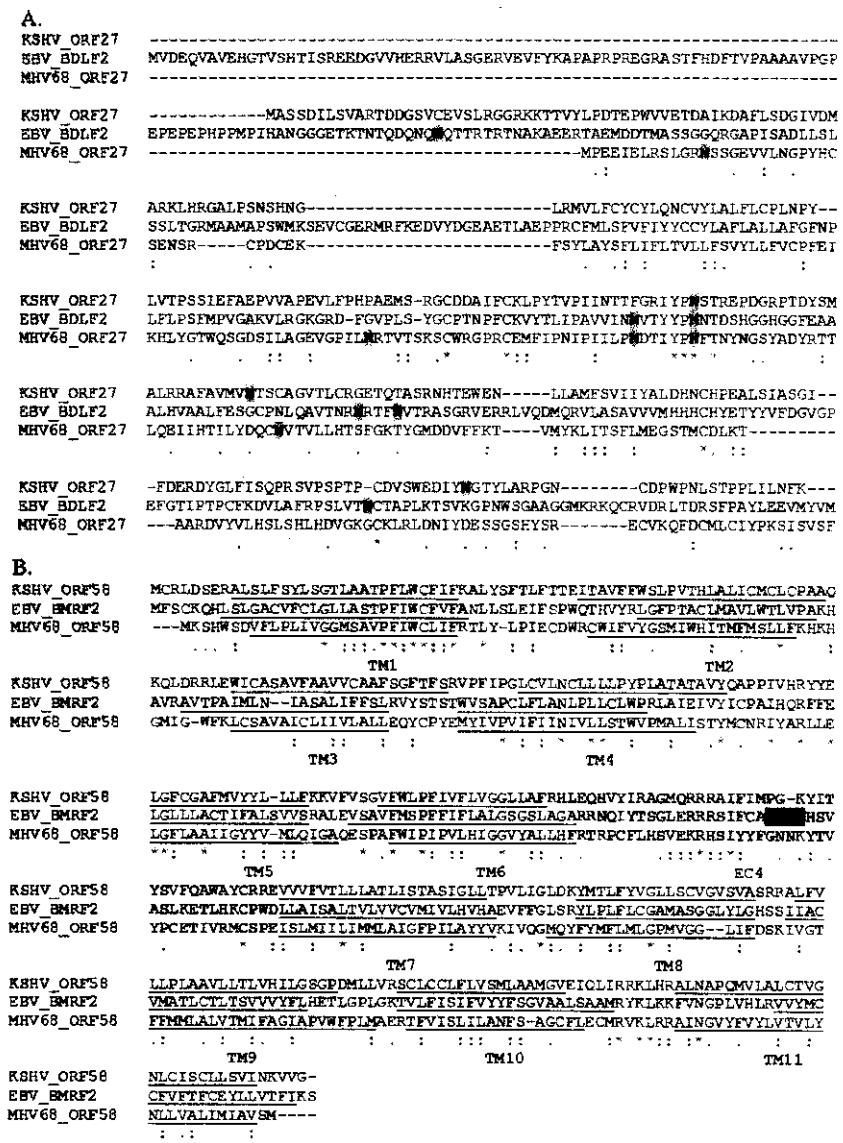

Figure 1. Sequence analysis of KSHV ORF27 and ORF58. Sequence analysis of KSHV ORF27 and ORF58 was performed using ClustalW2. **A.** Alignment results of MHV-68 (ORF27), KSHV (ORF27), and EBV (BDLF2). Identification of N-linked glycan attachment sites, highlighted in grey, were done using NetNGlyc 1.0 Server program. **B.** Alignment results of MHV-68 (ORF58), EBV (BMRF2), and KSHV (ORF58). Transmembrane regions were underlined for KSHV ORF58 and its homologues. Extracellular domain 4 (EC4) is highlighted in yellow and the RGD motif, within EC4, is highlighted in green.

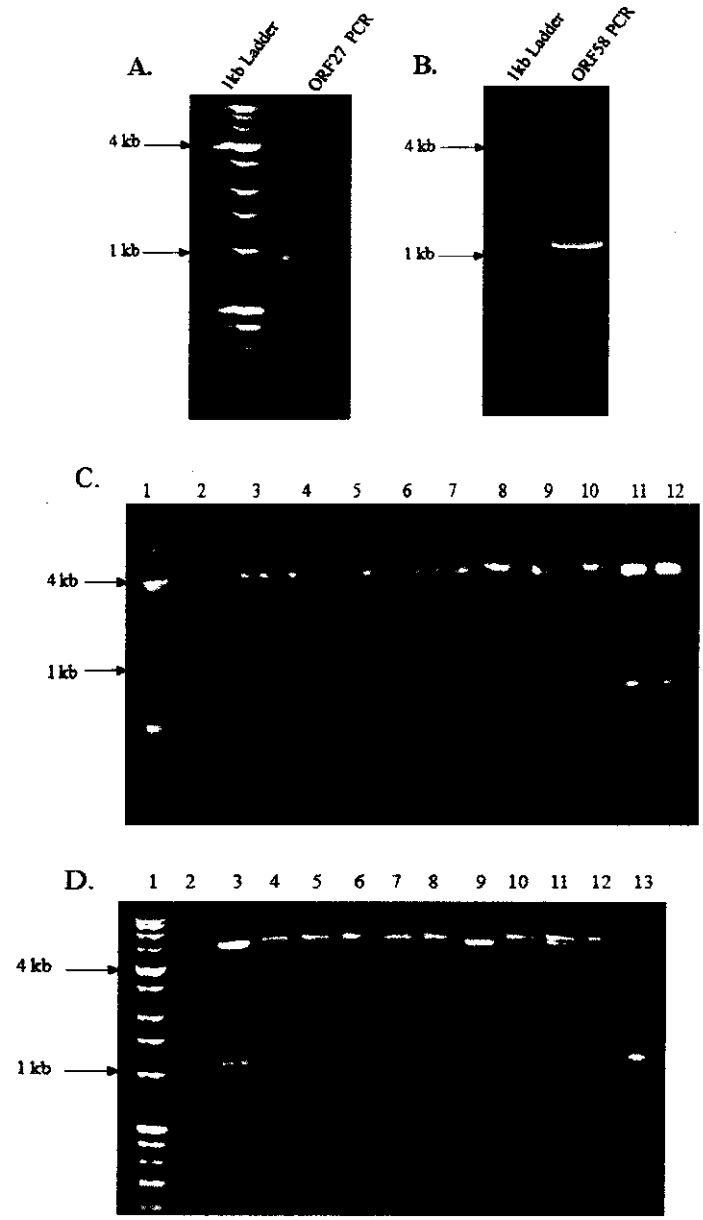

Figure 2: Cloning of phCMV2-ORF27 and p3XFLAG14-ORF58. A. PCR amplification of ORF27 using gene specific primers and BCBL-1 genomic DNA. **B.** PCR amplification product of ORF58. **C.** phCMV-2-ORF27 clones double digested with *EcoR* I and *Bgl* II. 1kb DNA ladder (lane 1), phCMV-2 control (lane 2), double digested clones 1-10 (lanes 3-12). **D.** p3XFLAG-14-ORF58 clones double digested with *EcoR* I and *Bgl* II. 1kb DNA ladder (lane 1), p3XFLAG-14 control (lane 2), double digested clones 1-10 (lanes 3-12), ORF58 insert control (lane 13).

identity, ORF27-C1 was used for subsequent analyses. The sequence results for KSHV ORF58-C3 and C8 revealed 96% identity to the published KSHV ORF58 sequence (accession number AAC57143.1) (data not shown).

Protein expression of KSHV ORF27 and ORF58 clones

To determine if protein expression would be observed, a western blot analysis was performed on ORF27 and ORF58 clones expressed in mammalian cells. The ORF27 insert was N-terminally tagged with an in-frame HA fusion protein. ORF58 was tagged with an in-frame 3XFLAG fusion protein. A total of three ORF58 constructs were created; they included an N-terminal 3XFLag tag, a 3XFLAG N- and Myc C-terminal tag and finally a 3XFLAG C-terminal tag insert. The phCMV2-ORF27 and p3XFLAG-ORF58 constructs were transfected into Vero cells, total protein was extracted, separated on a 10% SDS-PAGE gel, and western blot analysis was carried out. The expected size of the ORF27 fusion protein was 34.5kDa. In Figure 3A, a band of approximately 34.5 kDa was observed in lanes 4 and 5 indicating that ORF27 was successfully expressed from the phCMV2 plasmid. Some non-specific bands were also observed but the ORF27 bands were intense in comparison. A 41kDa band, which would correspond to the ORF58 fusion protein, was not observed (Figure 3B) (C-terminal tag). An intense band for the positive control FLAG-V-cyclin-C7 was observed in lane 4 verifying the transfection and western blot worked properly. Similar results were observed for all other ORF58 constructs (data not shown). The ORF58 fusion protein was never observed in any western blot analyses. Another mammalian cell line, 293T, was also used; however, expression of the ORF58 fusion protein was not observed (data not shown).

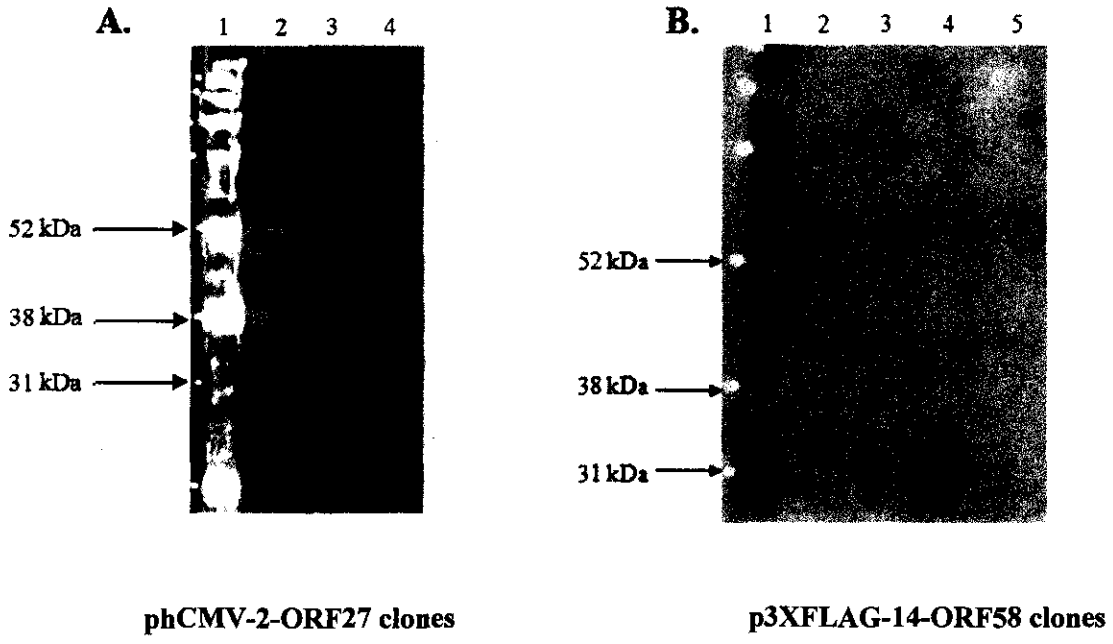

Figure 3. Protein expression of phCMV-2-ORF27 and p3XFLAG-14-ORF58. phCMV2-ORF27 and p3XFLAG-ORF58 clones were transfected into Vero cells, total protein was extracted, run on 10% SDS-PAGE gel and then analyzed via western blot. **A.** ORF27 protein expression. Full range rainbow GE Healthcare molecular weight marker (lane 1), negative control mock transfected Vero cells (lane 2), phCMV-2-ORF27-C1 (lane 3), phCMV-2-ORF27-C10 (lane 4). The expected size of the HA-ORF27 fusion protein was 34.5 kDa. **B.** ORF58 protein expression. Full range rainbow GE Healthcare molecular weight marker (lane 1), p3XFlag-14-ORF58-C3 C-term tag (lane 2), p3XFlag-14-ORF58-C8 C-term tag (lane 3), positive control v-Cyclin clone 7 (lane 4), negative control mock transfected Vero cells (lane 5). The expected size of the 3XFlag-ORF58 fusion protein was 41 kDa.

Detection of ORF58 mRNA by RT-PCR

To examine possible reasons why the ORF58 fusion protein was not expressed, total RNA of p3X-FLAG-ORF58 transfected cells were analyzed for the presence of ORF58 mRNA. Vero cells were transfected with ORF58 clones including N-terminal tag, C-and N-terminal tag, and C-terminal tag clones. Total RNA was isolated from the cells. Reverse transcriptase converted mRNA to cDNA. PCR was then carried out with gene specific primers to amplify the targeted DNA. As a control, the ORF58 samples were also run without RT (Figure 4A, lanes 8-13) which would identify DNA contamination in the isolated RNA samples. The ORF58 samples where mRNA was observed were the C-terminal tag (lanes 2-3) and the C- and N-terminal tag (lane 6) clones. In Figure 4B, GAPDH positive control bands were observed confirming that mRNA was properly reverse transcribed and amplified in all samples. The presence of ORF58 mRNA would indicate the DNA was being transcribed in the cell.

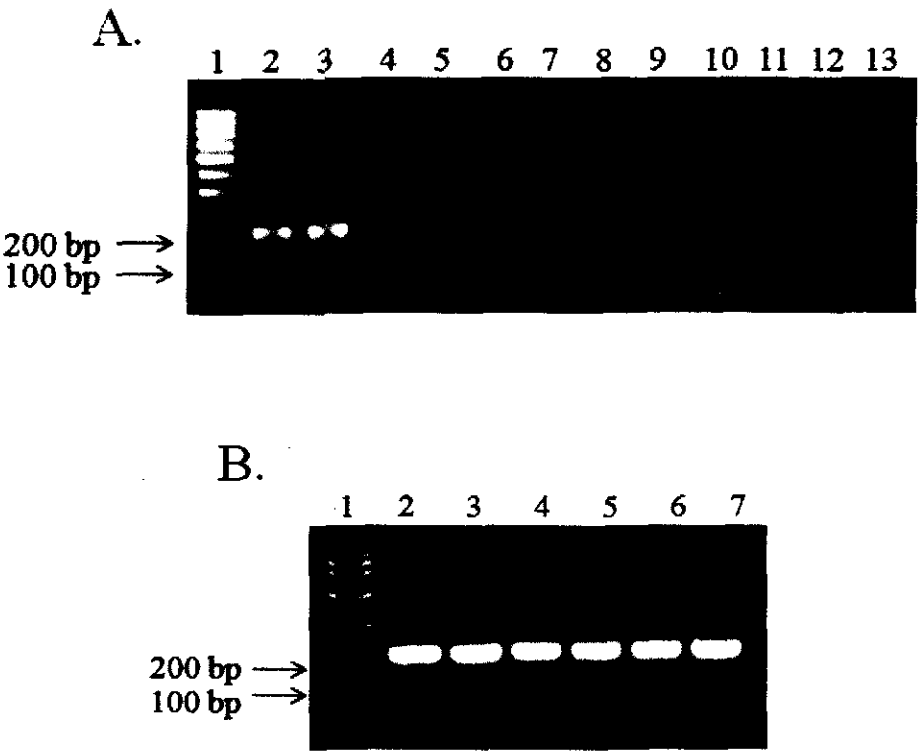

Figure 4. Detection of ORF58 mRNA with RT-PCR. P3XFLAG-ORF58 constructs were transfected into Vero cells, total RNA was collected and reverse transcription-PCR was performed. ORF58 RT-PCR product is 206 bp in length **A.** ORF58 RTPCR product run on agarose gel. 100bp DNA ladder (lane 1), p3XFLAG-14/26-ORF58 clones with RT (lanes 2-6), p3XFlag-14 vector with RT (lane 7), and control reactions without RT (lane 8-13). **B.** GAPDH primers were used as a positive control for all reactions with RT. 100bp DNA ladder (lane 1), p3XFLAG-14/26-ORF58 clones (lanes 2-6), p3XFlag-14 vector (lane 7).

ORF27 protein visualization by means of immunofluorescence

In order to visualize the localization of the KSHV ORF27 fusion protein an immunofluorescence assay was performed. After the expression of the ORF27 fusion protein was verified by western blot analysis, phCMV-2-ORF27-C1 clone was then transfected into Vero cells to determine sub-cellular localization of ORF27. Vero cells were grown onto coverslips and transfected with phCMV2-ORF27-C1 clone. Forty eight hours post-transfection cells were fixed, stained with specific antibodies, counter stained, and mounted onto slides. The cells were observed using a confocal microscope. ORF27 protein was observed throughout the cytoplasm of the cell (Figure 5A) and was not localized to the plasma membrane. This is similar to what Sander *et al.* (2008) observed for KSHV ORF27 localization. The phCMV2 control transfection showed no background immunofluorescence (Figure 5B).

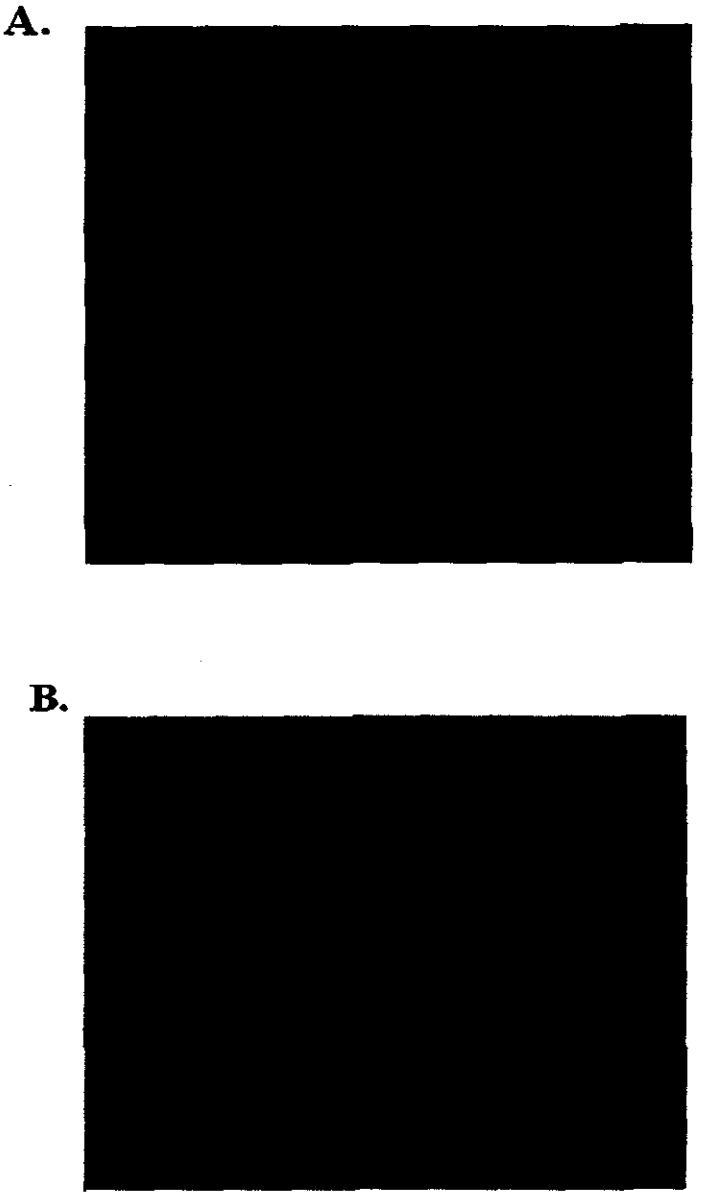

Figure 5. Expression of ORF27 in the Cytoplasm of Vero cells. Vero cells were grown onto coverslips and transfected with phCMV2-ORF27-C1. Cells were fixed in 3.7% paraformaldehyde, blocked in 1% BSA/PBS. Cells were stained with primary and secondary antibodies. The nuclei were counter stained with DAPI (blue). Coverslips were mounted and images were taken using a confocal microscope. **A.** HA-ORF27-C1 fusion protein (green), **B.** phCMV2 vector only control.

Discussion

KSHV was discovered by Chang *et al.* in 1994 and has since been found to be the cause of Kaposi's sarcoma, primary effusion lymphoma and multicentric Castleman's disease (Ablashi *et al.*, 2002). KSHV is an enveloped gamma herpesvirus with many different glycoproteins (Russo *et al.*, 1996). Enveloped viruses have a lipid layer that surrounds the nucleoprotein core; therefore, entry into the host cell requires either fusion between the cell membrane and the envelope or endocytosis of the virus into the cell (Greene *et al.*, 2009; Knipe *et al.*, 2001). Glycoproteins play a critical role in attachment, entry, and possibly virion egress (Chandran, 2010; Subramanian *et al.*, 2010). Consequently, it is vital that all known and any possible KSHV glycoproteins are examined to better understand the processes of entry and egress. KSHV ORF27 and ORF58 are possible glycoproteins but their functions are unknown (Chandran *et al.*, 1998; Russo *et al.*, 1996).

In this study we examined the localization of KSHV ORF27 and 58. It has been shown that the ORF27 and ORF58 homologues in both EBV and MHV-68 form a stable protein complex that co-localize at the plasma cell membrane when they were co-expressed (Loesing *et al.*, 2009; May *et al.*, 2005a). Both KSHV ORF27 and ORF58 were positively cloned into vectors for mammalian expression (Figures 2C and 2D). We attempted to observe the co-localization of KSHV ORF27 and ORF58 fusion proteins; however, we were unable to properly express the ORF58 fusion protein. The ORF27 fusion protein was successfully expressed and observed within the cytoplasm of

mammalian cells (Figure 3A and Figure 5A). Due to the lack of the ORF58 protein expression we were not able to examine the co-localization of KSHV ORF27 and ORF58 proteins.

When we examined the protein sequence alignment of ORF27 we noticed the differences in the length of the cytoplasmic tail for the ORF27 homologues (Figure 1A). The KSHV ORF27 cytoplasmic tail was 82 amino acids shorter than EBV BDLF2 and 32 amino acids longer than MHV-68 ORF27. No documentation has been published on the significance of the cytoplasmic tail length for KSHV ORF27 or EBV BDLF2. However, Gill *et al.* (2008) found that a truncated cytoplasmic tail of MHV-68 ORF27 stopped the creation of fronds. Fronds are finger like protrusions of the cell membrane that are created by actin rearrangement within the cell (Gill *et al.*, 2008). The many fronds increase the surface area and extend the cell membrane which may aid in viral infection to uninfected cells (Gill *et al.*, 2008). MHV-68 ORF27 and ORF58 induce actin rearrangement causing the creation of these fronds (Gill *et al.*, 2008). Therefore, the MHV-68 ORF27 cytoplasmic tail was needed for actin rearrangement (Gill *et al.*, 2008). The cytoplasmic tail is thought to interact with RhoA-dependent signaling pathways leading to actin polymerization (Gill *et al.*, 2008). Gill *et al.* (2008) also observed EBV BDLF2 and BMRF2 created similar fronds, but did not examine BDLF2 cytoplasmic tail truncation. Due to the similarity in the sequence analysis and the observations of Gill *et al.* (2008) for both MHV-68 ORF27 and EBV BDLF2, I would speculate the KSHV ORF27 cytoplasmic tail, which is shorter than BDLF2 and longer than MHV-68 ORF27, may also function in actin rearrangement.

In addition to attachment/entry, the MHV-68 ORF27 protein may also protect the EC4 region on the ORF58 protein from host antibodies (May *et al.*, 2005a). The extracellular domain of the MHV-68 ORF27 protein contains many N-linked glycosylation sites which, when heavily glycosylated, may assist in the protection of the EC4 region. The EC4 domain is similar to the RGD containing domain in EBV BMRF2 in that it can aid in binding to cells via cell surface integrins (May *et al.*, 2005a; Xiao *et al.*, 2009). The N-linked glycosylation sites were observed in the KSHV ORF27 and BDLF2 protein sequence alignment (Figure 1A) which suggests that the protein would also be glycosylated and possibly function to protect the EC4 domain in the ORF58 homologues. This protection would allow for the virus to evade the host immune system.

In the ORF58 protein sequence alignment we observed that all ORF58 homologues contained the 11 transmembrane domains. The RGD motif observed in the EC4 region of BMRF2, which is needed to bind to the basal membrane of polarized epithelial cells (Xiao *et al.*, 2007). The equivalent EC4 loop in MHV-68 ORF58 has been shown to bind to uninfected cell surfaces (May *et al.*, 2005a), but polarized cells were not specifically mentioned in the article. KSHV ORF58 does not contain an RGD motif in the EC4 region but there was high identity and conserved amino acids observed in the region. Due to the similarities observed in the sequences of the ORF58 homologues we would speculate that KSHV ORF58 would also aid in binding to the surface of host cells enabling cell to cell spread similar to what has been observed in both MHV-68 and EBV (May *et al.*, 2005a; Xiao *et al.*, 2007).

When KSHV ORF58 was not observed in western blot analysis we thought there could be a mutation occurring the in the clone DNA. The ORF58 constructs were transformed into *E. coli* DH5α cells. During replication a novel mutation may have been incorporated into the clone DNA, which could disrupt its protein expression. Mutation frequencies differ among *E. coli* strains and changing the *E. coli* strain used in transformation may lead to lower mutation frequency. Therefore, we transformed the p3XFLAG-14-ORF58 constructs into a different strain of *E. coli* called JM109 in an attempt to create clone DNA with fewer possible mutations. Clones created in the JM109 *E. coli* strain were transfected into mammalian cells, western blot analysis was performed and no protein bands were observed that would correspond to the ORF58 fusion protein (data not shown). We then looked into the placement of the tags. A C- or N-terminal tag may interfere with protein function and our construct was both C- and N-terminally tagged. We created new ORF58 constructs, an N-terminal tag and a C-terminal tag. Yet again, we did not observe protein on western blot analysis. Gore *et al.* (2008) observed problems with ORF58 protein expression on western blot which they attributed to the protein being highly hydrophilic. The researchers used a urea based SDS-PAGE gel and were able to observe the ORF58 protein (Gore *et al.*, 2009). We attempted to run the ORF58 clone protein extracts on a urea containing SDS-PAGE gel, but still did not observe expression of the fusion protein.

We then investigated ORF58 mRNA production within the transfected mammalian cells. If no mRNA was observed this would lead us to believe there was something wrong with transcription of the insert. We used RT-PCR to determine if

mRNA was produced. We found that mRNA was being transcribed for the C-terminal tag and the double tag constructs (Figure 4A). We speculate the problem of ORF58's protein expression could be due to degradation of a misfolded protein, or protein translation was halted for some reason. Further experiments need to be conducted to pin point the source of the problem.

Sander *et al.* (2007) determined the localization patterns of KSHV ORF27 and ORF58 following transfection of HeLa cells. ORF27 was observed throughout the cytoplasm heterogeneously (Sander *et al.*, 2007) similar to the localization we had observed for ORF27 (Figures 5A). MHV-68 ORF27 and BDLF2 were found to be expressed within the ER when transfected without the ORF58 homologues (Gore *et al.*, 2009; May *et al.*, 2005b). We observed similar a localization pattern in KSHV ORF27 which supports our theory that the protein would be found throughout the cytoplasm when transfected without KSHV ORF58. Sander *et al.* (2007) found ORF58 was subcellularly localized in the TGN. We theorized that ORF58 may be expressed if ORF27 was also present in the cell. In attempt to visualize the ORF58 fusion protein we co-transfected the ORF27 and 58 clones into mammalian cells, but ORF58 protein was still not observed (data not shown).

In conclusion, KSHV ORF27 was successfully cloned into the phCMV-2 vector. The gene was properly expressed in mammalian cells and observed via western blot analysis and by means of immunofluorescence. KSHV ORF27, when expressed alone, was observed in the cytoplasm of the cell and not on the cell surface as was hypothesized. The localization of KSHV ORF27 within the cell and not at the cell surface may mean

the protein was not fully processed; therefore, it could not be translocated to the cell surface. KSHV ORF58 was successfully cloned three times into the p3XFLAG vector, and was tagged at the C- and N- terminus, the C-terminus, and the N terminus. The RT-PCR experiment demonstrated that KSHV ORF58 mRNA was transcribed for some clones, but the other clones may have had mutations which did not allow for mRNA production. KSHV ORF58 protein was never observed on western blot analysis or immunofluorescence (data not shown). Future experiments would include looking at possible pathways of protein degradation for ORF58. If protein degradation can be halted then co-localization experiments can be carried out with co-transfection of KSHV ORF27. Finally, observing possible specific protein interactions between KSHV ORF27 and ORF58 would confirm they form a protein complex similar to that observed in EBV and MHV-68 (Loesing *et al.*, 2009; May *et al.*, 2005a).

Literature Cited

Ablashi D. V., L. G. Chatlynne, J. E. Whitman, and E. Cesarman. 2002. Spectrum of Kaposi's Sarcoma-Associated Herpesvirus, or Human Herpesvirus 8, Diseases. Clinical Microbiology Reviews **15**:439-464.

Akula S. M., F. Z. Wang, J. Vieira, and B. Chandran. 2001. Human herpesvirus 8 interaction with target cells involves heparan sulfate. Virology **282**:245-255.

Akula S. M., N. P. Pramod, F. Z. Wang, and B. Chandran. 2002. Integrin alpha3beta1 (CD 49c/29) is a cellular receptor for Kaposi's sarcoma-associated herpesvirus (KSHV/HHV-8) entry into the target cells. Cell **108**:407-419.

Akula S. M., P. P. Naranatt, N. Walia, F. Wang, B. Fegley, and B. Chandran. 2003. Kaposi's Sarcoma-Associated Herpesvirus (Human Herpesvirus 8) Infection of Human Fibroblast Cells Occurs through Endocytosis. Journal of Virology **77**:7978-7990.

Birkmann A., K. Mahr, A. Ensser, S. Yaguboglu, F. Titgemeyer, B. Fleckenstein, and F. Neipel. 2001. Cell Surface Heparan Sulfate Is a Receptor for Human Herpesvirus 8 and Interacts with Envelope Glycoprotein K8.1. Journal of Virology **75**:11583-11593.

Blom N., T. Sicheritz-Pontén, R. Gupta, S. Gammeltoft, and S. Brunak. 2004. Prediction of post-translational glycosylation and phosphorylaation of proteins from the amino acid sequence. Proteomics **4**:1633-1649.

Chandran B. 2010. Early Events in Kaposi's Sarcoma-Associated Herpesvirus Infection of Target Cells. Journal of Virology **84**:2188-2199.

Chandran B., C. Bloomer, S. R. Chan, L. Zhu, E. Goldstein, and R. Horvat. 1998. Human Herpesvirus-8 ORF K8.1 Gene Encodes Immunogenic Glycoproteins Generated by Spliced Transcripts. Virology **249**:140-149.

Chen J., F. Ye, J. Xie, K. Kuhne, and S. Gao. 2009. Genome-wide identification of binding sites for Kaposi's sarcoma-associated herpesvirus lytic switch protein, RTA. Virology **386**:290-302.

Chen Y., A. Rahemtullah, and E. Hochberg. 2007. Primary Effusion Lymphoma. Oncologist **12**:569-576.

Chenna R., H. Sugawara, T. Koike, R. Lopez, T. J. Gibson, D. G. Higgins, and J. D. Thompson. 2003. Multiple sequence alignment with the Clustal series of programs. Nucleic Acids Research **31**:3497-3500.

De Clercq E. 2003. Clinical Potential of the Acyclic Nucleoside Phosphonates Cidofovir, Adefovir, and Tenofovir in Treatment of DNA Virus and Retrovirus Infections. Clinical Microbiology Reviews **16**:569-596.

Dourmishev L. A., A. L. Dourmishev, D. Palmeri, R. A. Schwartz, and D. M. Lukac. 2003. Molecular Genetics of Kaposi's Sarcoma-Associated Herpesvirus (Human Herpesvirus 8) Epidemiology and Pathogenesis. Microbiology and Molecular Biology Reviews **67**:175-212.

Ebrahimi B., B. M. Dutia, K. L. Roberts, J. J. Garcia-Ramirez, P. Dickinson, J. P. Stewart, P. Ghazal, D. J. Roy, and A. A. Nash. 2003. Transcriptome profile of murine gammaherpesvirus-68 lytic infection. Journal of General Virology **84**:99-109.

Gill M. B., R. Edgar, J. S. May, and P. G. Stevenson. 2008. A Gamma-Herpesvirus Glycoprotein Complex Manipulates Actin to Promote Viral Spread. PLoS ONE **3**:e1808.

Gore M., and L. M. Hutt-Fletcher. 2009. The BDLF2 protein of Epstein-Barr virus is a type II glycosylated envelope protein whose processing is dependent on coexpression with the BMRF2 protein. Virology **383**:162-167.

Greene W., and S. Gao. 2009. Actin Dynamics Regulate Multiple Endosomal Steps during Kaposi's Sarcoma-Associated Herpesvirus Entry and Trafficking in Endothelial Cells. PLoS Pathog **5**.

Greene W., K. Kuhne, F. Ye, J. Chen, F. Zhou, X. Lei, and S. Gao. 2007. Molecular biology of KSHV in relation to AIDS-associated oncogenesis. Cancer Treatment and Research **133**:69-127.

Hengge U., T. Ruzicka, S. Tyring, M. Stuschke, M. Roggendorf, R. Schwartz, and S. Seeber. 2002. Update on Kaposi's sarcoma and other HHV8 associated diseases. Part 2: pathogenesis, Castleman's disease, and pleural effusion lymphoma. The Lancet Infectious Diseases **2**:344-352.

Hengge U. R., T. Ruzicka, S. K. Tyring, M. Stuschke, M. Roggendorf, R. A. Schwartz, and S. Seeber. 2002. Update on Kaposi's sarcoma and other HHV8 associated diseases. Part 1: epidemiology, environmental predispositions, clinical manifestations, and therapy. The Lancet Infectious Diseases **2**:281-292.

Jenner R. G., and C. Boshoff. 2002. The molecular pathology of Kaposi's sarcoma associated herpesvirus. Biochimica et Biophysica Acta (BBA) - Reviews on Cancer **1602**:1-22.

Johannsen E., M. Luftig, M. R. Chase, S. Weicksel, E. Cahir-McFarland, D. Illanes, D. Sarracino, and E. Kieff. 2004. Proteins of purified Epstein-Barr virus. Proceedings of the National Academy of Sciences of the United States of America **101**:16286-16291.

Knipe D. M., and P. M. Howley. 2001. Fields VirologyFourth Edition. Lippincott Williams & Wilkins.

Lint, A.L., D.M. Knipe. 2009. Herpespviruses, pp. pp. 376-90. *In* Encyclopedia of Microbiology, M. Schaechter editor, Elsevier, Oxford.

Loesing J., S. Di Fiore, K. Ritter, R. Fischer, and M. Kleines. 2009. Epstein-Barr virus BDLF2-BMRF2 complex affects cellular morphology. Journal of General Virology **90**:1440-1449.

Lu M., J. Suen, C. Frias, R. Pfeiffer, M. Tsai, E. Chuang, and S. L. Zeichner. 2004. Dissection of the Kaposi's Sarcoma-Associated Herpesvirus Gene Expression Program by Using the Viral DNA Replication Inhibitor Cidofovir. Journal of Virology **78**:13637-13652.

May J. S., B. D. de Lima, S. Colaco, and P. G. Stevenson. 2005. Intercellular Gamma Herpesvirus Dissemination Involves Co-Ordinated Intracellular Membrane Protein Transport. Traffic **6**:780-793.

May J. S., J. Walker, S. Colaco, and P. G. Stevenson. 2005. The Murine Gammaherpesvirus 68 ORF27 Gene Product Contributes to Intercellular Viral Spread. Journal of Virology **79**:5059-5068.

Nakamura H., M. Lu, Y. Gwack, J. Souvlis, S. L. Zeichner, and J. U. Jung. 2003. Global Changes in Kaposi's Sarcoma-Associated Virus Gene Expression Patterns following Expression of a Tetracycline-Inducible Rta Transactivator. Journal of Virology 77:4205-4220.

Naranatt P. P., H. H. Krishnan, M. S. Smith, and B. Chandran. 2005. Kaposi's Sarcoma-Associated Herpesvirus Modulates Microtubule Dynamics via RhoA GTP-Diaphanous 2 Signaling and Utilizes the Dynein Motors To Deliver Its DNA to the Nucleus. Journal of Virology **79**:1191-1206.

Pelser C., F. Vitale, D. Whitby, B. I. Graubard, A. Messina, L. Gafà, E. E. Brown, L. A. Anderson, N. Romano, C. Lauria, and J. J. Goedert. 2009. Socio-economic and other correlates of Kaposi sarcoma-associated herpesvirus seroprevalence among older adults in Sicily. Journal of Medical Virology **81**:1938-1944.

Pyakurel P., F. Pak, A. Mwakigonja, E. Kaaya, and P. Biberfeld. 2007. KSHV/HHV 8 and HIV infection in Kaposi's sarcoma development. Infectious Agents and Cancer **2**:4.

Raghu H., N. Sharma-Walia, M. V. Veettil, S. Sadagopan, and B. Chandran. 2009. Kaposi's Sarcoma-Associated Herpesvirus Utilizes an Actin Polymerization Dependent Macropinocytic Pathway To Enter Human Dermal Microvascular Endothelial and Human Umbilical Vein Endothelial Cells. Journal of Virology **83**:4895-4911.

Rappocciolo G., F. J. Jenkins, H. R. Hensler, P. Piazza, M. Jais, L. Borowski, S. C. Watkins, and C. R. Rinaldo. 2006. DC-SIGN Is a Receptor for Human Herpesvirus 8 on Dendritic Cells and Macrophages. Journal of Immunology **176**:1741-1749.

Rossetto C., Y. Gao, I. Yamboliev, I. Papouskova, G. Pari. 2007. Transcriptional repression of K-Rta by Kaposi's sarcoma-associated herpesvirus K-bZIP is not required for oriLyt-dependent DNA replication. Virology **369**:340–350.

Russo J., R. Bohenzky, M. Chien, J. Chen, M. Yan, D. Maddalena, J. Parry, D. Peruzzi, I. Edelman, Y. Chang, and P. Moore. 1996. Nucleotide sequence of the Kaposi sarcoma-associated□herpesvirus□(HHV8). Proceedings of the National Academy of Sciences of the United States of America **93**:14862-14867.

Sander G., A. Konrad, M. Thurau, E. Wies, R. Leubert, E. Kremmer, H. Dinkel, T. Schulz, F. Neipel, and M. Sturzl. 2007. Intracellular Localization Map of HHV-8 Proteins. Journal of Virology JVI.01716-07.

Sharma-Walia N., H. Raghu, S. Sadagopan, R. Sivakumar, M. V. Veettil, P. P. Naranatt, M. M. Smith, and B. Chandran. 2006. Cyclooxygenase 2 Induced by Kaposi's Sarcoma-Associated Herpesvirus Early during In Vitro Infection of Target Cells Plays a Role in the Maintenance of Latent Viral Gene Expression. Journal of Virology **80**:6534-6552.

Subramanian R., I. Sehgal, O. D'Auvergne, and K. G. Kousoulas. 2010. Kaposi's sarcoma-associated herpesvirus glycoproteins B and K8.1 regulate virion egress and synthesis of vascular endothelial growth factor and viral interleukin-6 in BCBL-1 cells. Journal of Virology **84**:1704-1714.

Tarbouriech N., M. Buisson, T. Géoui, S. Daenke, S. Cusack, and W. P. Burmeister. 2006. Structural genomics of the Epstein–Barr virus. Acta Crystallographica Section D: Biological Crystallography **62**:1276-1285.

Veit M., E. Ponimaskin, S. Baiborodin, H. R. Gelderblom, and M. F. G. Schmidt. 1996. Intracellular compartmentalization of the glycoprotein B of herpesvirus Simian agent 8 expressed with a baculovirus vector in insect cells. Archives of Virology **141**:2009-2017.

Verschuren E. W., N. Jones, and G. I. Evan. 2004. The cell cycle and how it is steered by Kaposi's sarcoma-associated herpesvirus cyclin. Journal of General Virology **85**:1347-1361.

Wen K. W., and B. Damania. 2010. Kaposi sarcoma-associated herpesvirus (KSHV): Molecular biology and oncogenesis. Cancer Letters **289**:140-150.

Xiao J., J. M. Palefsky, R. Herrera, J. Berline, and S. M. Tugizov. 2009. EBV BMRF-2 facilitates cell-to-cell spread of virus within polarized oral epithelial cells. Virology **388**:335-343.

Xiao J., J. M. Palefsky, R. Herrera, J. Berline, and S. M. Tugizov. 2008. The Epstein Barr Virus BMRF-2 Protein Facilitates Virus Attachment to Oral Epithelial Cells. Virology **370**:430-442.

Xiao J., J. M. Palefsky, R. Herrera, and S. M. Tugizov. 2007. Characterization of the Epstein-Barr virus glycoprotein BMRF-2. Virology **359**:382-396.

Yoo S. M., F. Zhou, F. Ye, H. Pan, and S. Gao. 2005. Early and sustained expression of latent and host modulating genes in coordinated transcriptional program of KSHV productive primary infection of human primary endothelial cells. Virology **343**:47-64.

Zhu F. X., J. M. Chong, L. Wu, and Y. Yuan. 2005. Virion Proteins of Kaposi's Sarcoma-Associated Herpesvirus. Journal of Virology **79**:800-811.

Zhu F. X., S.M. King, E.J. Smith, D.E. Levy, Y. Yuan. 2002. A Kaposi's sarcoma associated herpesviral protein inhibits virus-mediated induction of type I interferon by blocking IRF-7 phosphorylation and nuclear accumulation. Proceeding of the National Academy of Sciences USA **99**:5573–5578.